Core Instability and Spatiotemporal Intermittency of Spiral Waves in Oscillatory Media

Igor Aranson,[1] Lorenz Kramer,[2] and Andreas Weber[2]
[1]*Department of Physics, Bar-Ilan University, Ramat Gan, 52900, Israel*
[2]*Physikalisches Institut der Universität Bayreuth, 95440 Bayreuth, Germany*
(Received 3 September 1993)

We show that in a parameter range which is important in particular for optical instabilities spiral waves in the complex (generalized) Ginzburg-Landau equation are unstable with respect to a core instability which leads to spontaneous acceleration of the spiral. Depending on the parameters the system settles down in at least four qualitatively different spatiotemporally chaotic states.

PACS numbers: 05.45.+b, 47.20.-k

The complex Ginzburg-Landau equation (CGLE),

$$\partial_t A = A + (\varepsilon + i)\Delta A - (1 + ic)|A|^2 A, \qquad (1)$$

has become very popular in recent years (note that in the more usual scaling one has length rescaled by $\sqrt{\varepsilon}$ and $\varepsilon = 1/|b|$). It describes the slowly varying amplitude and phase of a mode which bifurcates supercritically via an oscillatory instability (Hopf bifurcation) from a homogeneous state [1]. Examples of such media are chemical oscillations and anisotropic systems sustaining (nonlinear) traveling waves, e.g., convection instabilities in nematic liquid crystals (for general reviews see [2]). Transversely extended lasers or passive nonlinear media are other systems where the oscillatory instability occurs [3]. In this case systematic derivation of the CGLE from the Maxwell-Bloch equations in the "good cavity limit" for positive detuning between the cavity resonance and the atomic line [4–6] leads to very small values of $\varepsilon \sim 10^{-3}$–10^{-2} [6].

Equation (1) has plane-wave solutions $A = \sqrt{1-\varepsilon k^2}\exp\{i[\omega t + \mathbf{k}\cdot\mathbf{r}]\}$ with $\omega = -k^2 - c(1-\varepsilon k^2)$ and $k^2 < 1/\varepsilon$. They are stable within a narrower k band as long as $\varepsilon + c > 0$ holds. For $k \neq 0$ one has first the onset of the convective Eckhaus instability and subsequently absolute instability [7].

More general solutions involve topological point defects in 2D (and line defects in 3D) which correspond to simple zeros of A. One has topological quantum numbers ± 1 related to the phase change of $\pm 2\pi$ when going around the defect. When $c \neq 1/\varepsilon$ the defects are usually sources of spiral waves whose constant phase lines behave like an Archimedean spiral, except in the immediate neighborhood of the core. The stationary one-armed (or singly charged) isolated spiral solution of Eq. (1) is of the form

$$A(r,\theta) = F(r)\exp\{i[\omega t \pm \theta + \psi(r)]\}\,, \qquad (2)$$

where (r,θ) are polar coordinates. The real functions F and ψ have the following asymptotic behavior: $F(r) \to \sqrt{1-\varepsilon k^2}\,, \psi'(r) \to k$ for $r \to \infty$ and $F(r) \sim r\,, \psi'(r) \sim r$ for $r \to 0$. The wave number k of the asymptotic waves emitted by the spiral is determined uniquely for given ε, c. In general k has to be determined numerically [8].

For $\varepsilon \neq 0$ the rigidly rotating solutions of Eq. (1) can be obtained by a similarity transformation [7,8] from the case $\varepsilon = 0$ with a transformed value of c given by $\tilde{c} = (c+\varepsilon)(1-\varepsilon c)$.

For $\varepsilon = 0$ one has a type of Galilean invariance (see [9] for the 1D case) and then in addition to the stationary spiral there exists a family of spirals moving with arbitrary constant velocity $\mathbf{v}$

$$A(r,t) = F(r')\exp\left(i\left[\omega' t + \theta + \psi(r') - \frac{\mathbf{r}'\cdot\mathbf{v}}{2}\right]\right)\,, \qquad (3)$$

where $\mathbf{r}' = \mathbf{r} + \mathbf{v}t$, $\omega' = \omega + v^2/4$, and the functions F, ψ are those of Eq. (2) (this invariance holds for any stationary solution). For $\varepsilon \neq 0$ the diffusion term $\sim \varepsilon\Delta A$ destroys the family and in fact leads to acceleration of the spiral proportional to εv. The usual (tacit) assumption is that the stationary spiral, which survives the perturbation, is in fact stable [6]. We show here that this is not the case, and that stable spirals exist only above some critical value ε_c. Below ε_c the stationary spirals are unstable with respect to spontaneous acceleration. To demonstrate these statements we adopted an analytic method and performed direct numerical simulations.

First we consider the limit $0 < \varepsilon \ll 1$. For small values of ε one may expect the solution (3) to be slightly perturbed and have a slowly varying velocity $\mathbf{v}$ which obeys an equation of motion of the form $\partial_t \mathbf{v} + \varepsilon\hat{K}\mathbf{v} = 0$. Because of isotropy the elements of the tensor $\hat{K}$ must satisfy $K_{11} = K_{22}$ and $K_{12} = -K_{21}$, so the relation can also be written as

$$\partial_t \hat{v} + \varepsilon\kappa\hat{v} = 0, \qquad (4)$$

where $\hat{v} = v_y + iv_x$ and $\kappa = K_{11} - iK_{12}$. Since in general the friction constant κ is complex, the spiral core moves on a (logarithmic) spiral trajectory.

Perturbed solutions with slowly varying velocity can be written as

$$A(r,t) = [F(r') + W]\exp\left(i\left[\omega' t + \theta + \psi(r') - \frac{\mathbf{r}'\cdot\mathbf{v}}{2}\right]\right). \qquad (5)$$

Separating real and imaginary parts of W, representing it in the form of a Fourier series

0031-9007/94/72(15)/2316(4)$06.00

$$\begin{pmatrix}\mathrm{Re}W\\ \mathrm{Im}W\end{pmatrix}=\sum_{n=-\infty}^{\infty}\begin{pmatrix}A_n(r)\\ B_n(r)\end{pmatrix}\exp(in\theta)\,, \tag{6}$$

and assuming $|v|,\varepsilon\ll 1$, one obtains from Eq. (1) a set of decoupled equations for each Fourier component. The acceleration appears only in the equations for $n=\pm 1$. We need only $n=1$ which is given by (after omitting primes on r)

$$\hat{\Delta}A_1-2\left(cF^2A_1+\psi' F\frac{\partial}{\partial r}\frac{B_1}{F}+\frac{iB_1}{r^2}\right)=\frac{\varepsilon\hat{v}}{2i}F'-\frac{r\partial_t\hat{v}}{4i}F\,, \tag{7}$$

$$\hat{\Delta}B_1+2\left(F^2A_1+\psi' F\frac{\partial}{\partial r}\frac{A_1}{F}+\frac{iA_1}{r^2}\right)=\frac{\varepsilon\hat{v}}{2i}\left(F\psi'+\frac{iF}{r}\right)\,,$$

where $\hat{\Delta}=\Delta_r-r^{-2}-\Delta_r F/F$, $\Delta_r=\partial_r^2+r^{-1}\partial_r$; primes now denote differentiation with respect to r. Actually the right hand side (r.h.s.) of Eqs. (7) diverges due to the acceleration term $r\partial_t\hat{v}$. This means that the *ansatz* (5) with $|W|$ small cannot be valid arbitrarily far away from the core. In fact the region of validity is large for small acceleration. In the outer region $r\partial_t v\gg 1$ the structure of the field A must be matched with the field described by (7), but it is not necessary to actually perform the matching in order to determine the acceleration. It suffices to adjust the value of the acceleration in such a (unique) way that the exponential growth, which is characteristic for generic solutions of Eqs. (7) with regular behavior at $r=0$, is suppressed, leading to more slow, in comparison to the exponential, powerlike growth. Since the r.h.s. of Eq. (7) is linear in $\hat{v}$ and $\partial_t\hat{v}$ one can proceed as follows (for more details see Ref. [10]).

The solutions of Eq. (7) are for large r in general dominated by two exponents with a positive real part, which are complex conjugated in the "oscillatory range" $(c+\varepsilon)/(1-c\varepsilon)<c_0=1.18$ (below curve OR in Fig. 1) and real otherwise ("monotonic range"). One computes numerically the (complex) prefactors C_{1v},C_{2v} of the two diverging exponents of an inhomogeneous solution for the choice $\hat{v}=1,\partial_t\hat{v}=0$ and similarly the constants C_{1a},C_{2a} for the choice $\hat{v}=0,\partial_t\hat{v}=1$ with the conditions $A_1(0)=B_1(0)=0$. Moreover, one calculates the prefactors $C_{1,2}$ of a homogeneous solution of Eq. (7) which is regular at $r=0$. Actually this regularity condition allows for two linearly independent homogeneous solutions, but one of them remains bounded for $r\to\infty$ and does not contribute to $C_{1,2}$ (see Ref. [10]). To obtain the solution of Eq. (7) with balanced exponential growth one has to adjust $\hat{v},\partial_t\hat{v}$, i.e., the inhomogeneities in Eq. (7), and the prefactor ξ of the homogeneous solution such that the relation

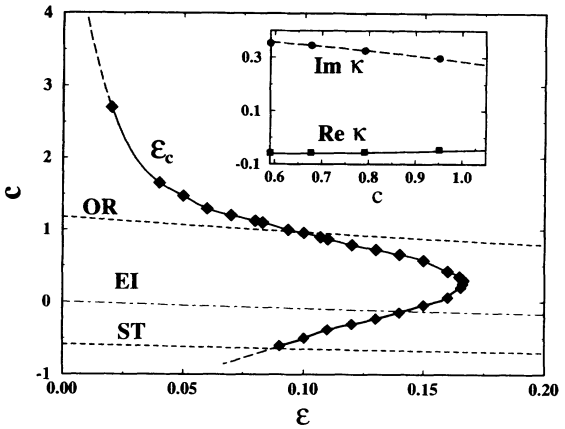

FIG. 1. Stability limits of spiral wave. ε_c is the core stability limit (unstable to the left), below EI is the Eckhaus unstable region, ST designates the transition line to "strong" turbulence, and below OR is the oscillatory range. The lines EI and OR are obtained by the linear stability analysis of outcoming waves. The line ST is obtained from the numerical solution of quasi-1D CGLE (see text below). Inset: Real and imaginary parts of κ versus c. The lines represent the analytical results; the symbols are obtained from 2D simulations for $\varepsilon=0.025$.

$$\xi\begin{pmatrix}C_1\\ C_2\end{pmatrix}+\partial_t\hat{v}\begin{pmatrix}C_{1a}\\ C_{2a}\end{pmatrix}+\hat{v}\begin{pmatrix}C_{1v}\\ C_{2v}\end{pmatrix}=0 \tag{8}$$

is satisfied. Eliminating ξ we obtain the relation (4) with $\varepsilon\kappa=(C_{1v}/C_1-C_{2v}/C_2)/(C_{1a}/C_1-C_{2a}/C_2)$. In this way we find that for $\varepsilon\to 0$ the real part of κ is always negative. The results for κ from the asymptotic analysis are in reasonable agreement with direct numerical simulations of the CGLE (see Fig. 1, inset). In the monotonic range the analysis is complicated by the fact that the exponents may be very different.

The acceleration instability of the spiral core has a well-known counterpart in excitable media, where the spiral "tip" can perform a quasiperiodic motion leading to meandering [11]. The main difference between the two cases is simple: In excitable media the nonlinear corrections to Eq. (4), which may be written in the form $\partial_t\hat{v}+\varepsilon\kappa\hat{v}=f(|\hat{v}|^2)\hat{v}$ with $f(0)=0$, has typically a negative real part and provides saturation of the instability, whereas in the CGLE the sign of $\mathrm{Re}f(|\hat{v}|^2)$ is opposite and does not lead to saturation according to the simulations. Thus we have found an alternative version of the meandering instability [11]. The scenario appears to be generic and cannot be destroyed by small perturbations of the CGLE.

Now going to larger ε one finds that $\mathrm{Re}\kappa$ increases with ε and finally changes sign at a value ε_c. The result is shown in Fig. 1. It is obtained from extensive numerical simulations of the CGLE on a CRAY 2 YMP supercomputer. We measured systematically $\mathrm{Re}\kappa$ above and below the curve. The zero of $\mathrm{Re}\kappa$ was then determined by linear interpolation.

We note that the acceleration instability can be interpreted as the destabilization of a localized core mode similar to the situation of the standing hole solution in the 1D CGLE [12,13]. The spatial decay rate $\sim \varepsilon$ of the mode is related to the time exponent $\varepsilon\kappa$ via the dispersion relation for plane waves.

The instability of the spiral core persists in the limit of the "defocusing" nonlinear Schrödinger equation, which corresponds to $c \to \infty$, $\varepsilon \to 0$ and falls into the monotonic range. In this limit $\psi \to 0$. The acceleration can in principle be found from the solvability conditions by projecting Eq. (1) onto the translation mode of the adjoint linearized operator. However, in that limit the integrals in the solvability condition diverge logarithmically. Introducing an appropriate cutoff one easily sees that κ becomes real, but its actual value is difficult to determine. Thus, in this limit the trajectory of the accelerating core is just a straight line.

Our result can also explain complex motion of the spiral core observed recently in the presence of a localized inhomogeneity [14] or with obstacles [15]. Although this motion was obtained in the stable range $\mathrm{Re}\kappa > 0$ ($\varepsilon > \varepsilon_c$), the external forces created by the inhomogeneity can excite the weakly damped core mode. Then the equation of motion for the spiral core will be of the form $\partial_t \hat{v} + \varepsilon\kappa\hat{v} = \mathbf{G}(\mathbf{r})$. The trajectory of this equation may perform complex motion even for very simple forms of the force term $\mathbf{G}(\mathbf{r})$. In fact, we found meandering-type motion for purely radial $\mathbf{G}(|\mathbf{r}|)$ [14].

Let us now discuss the typical behavior of the system when small random initial conditions are applied. Because of the extended parameter space and large CPU time requirements for reliable simulations our investigations should be considered as yet preliminary. Clearly one expects that for $\varepsilon < \varepsilon_c$ a state with persistent defects should be typically turbulent (spatiotemporal chaos). In the monotonic range (Fig. 1, above curve OR), this turbulence is characterized by fast motion of the defects (these defects are not really spirals because the asymptotic radiation field is not developed) and collisions, which often do not result in annihilation, in contrast to the case of the usual defect-mediated turbulence [16,17], where the waves emitted by the spiral are unstable. In Fig. 2, the number n of defects as a function of time is shown for a fairly large system (150 × 150). Apart from the rapid fluctuations due to creation and annihilation there is an extremely slow decrease of n (due to CPU time limitations we have not continued the simulations). The (quasi)stationary distribution is well described by $p(n) \sim \exp[-(n-\bar{n})^2/\bar{n}]$, where $\bar{n}$ is the average number of defects. The formula follows in the limit $n \to \infty$ from treating defect pairs as statistical independent entities [17]. Note that this assumption is strictly valid only for the full system. Otherwise the statistics is influenced by single defects entering or leaving the subsystem. When these processes dominate the exponent acquires a factor $\frac{1}{2}$. Actually, when crossing ε_c in the monotonic range the

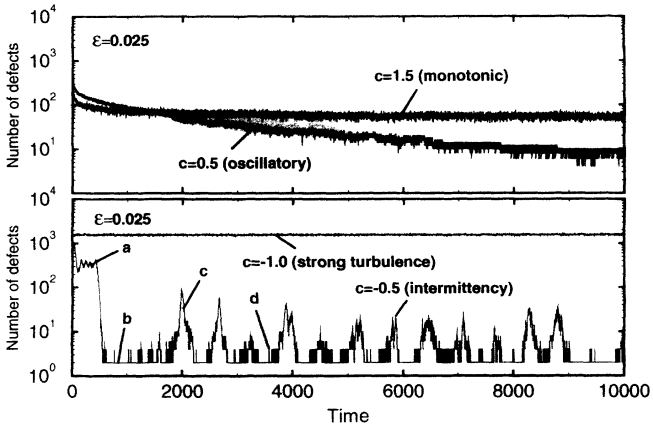

FIG. 2. The number of defects versus time for four different values of c and $\varepsilon = 0.025$. Parameters of the simulations are as follows: the domain of integration 150 × 150, the number of Fourier harmonics 256 × 256, the time step 0.02.

disordered state appears to persist (or is at least very long lived). Thus the single-spiral instability has presumably limited relevance for the collective behavior.

In the oscillatory range (Fig. 1, below curve OR) the behavior is drastically different. In the beginning of the process one has the formation of many spirals and the subsequent development of spontaneous symmetry breaking resulting in one spiral becoming dominant at least in not too large cells similar to the case $\varepsilon > \varepsilon_c$ (see Ref. [18] and Fig. 2). However, now the dominant spiral is unstable with respect to acceleration, resulting in continued motion of the core restricted by the shocks. Additional spirals are created only rarely. In very large systems one might expect a "dynamic vortex glass" [19].

When the Eckhaus instability of emitted plane waves sets in below curve EI of Fig. 1 the perturbations produced by the accelerating core of the dominant spiral are amplified away from the core due to the convective character of the instability. Eventually some critical level is exceeded, the state loses stability, and many new defects are created throughout the cell. Then the process repeats (Figs. 2 and 3). Such phenomena are very similar to spatiotemporal intermittency of holes observed in the 1D CGLE [13,20] and might be called *defect-mediated intermittency*. In a very large cell one expects to have such processes developing independently in different places of the cell, so one has persistent turbulent bursts (or spots) on the background of growing spirals. For $\varepsilon > \varepsilon_c$ the intermittency vanishes and then the curve EI plays no direct role.

Below curve ST in Fig. 1 the "strong" turbulence characteristic for the intermittent bursts becomes persistent ($\varepsilon < \varepsilon_c$). This turbulence is characterized by strong variations of the amplitude A everywhere in the domain. The defects play a passive role because the asymptotic waves are not emitted by the cores. This regime is similar to usual defect-mediated turbulence [16,17]. The curve ST

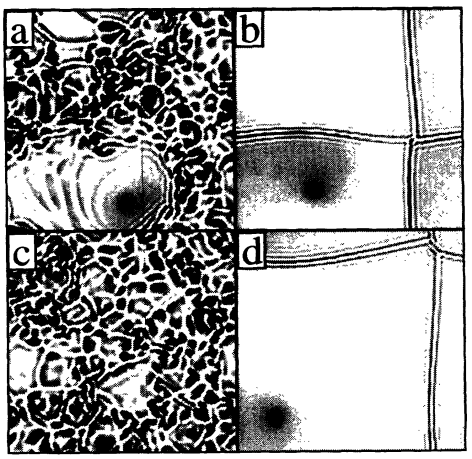

FIG. 3. Snapshots of $|A(x,y)|$ in the intermittency range for four consecutive times [$c = -0.5, \varepsilon = 0.025$; black: $|A(x,y)| = 0$; white: $|A(x,y)| = 1$]. The times corresponding to (a), (b), (c), and (d) are indicated in Fig. 2 .

lies slightly above the limit of absolute instability (see Ref. [7]) obtained from linear perturbation analysis of the selected wave number k. This analysis gives for $\varepsilon \to 0$ the value $c \approx -1.2$. Whereas spirals are indeed linearly stable up to the absolute stability limit their domain of attraction appears to become small below the curve ST. The curve was actually determined by simulating Eq. (1) with the restricted angular dependence (2) and boundary conditions $A(0) = 0, \partial_r A(L) = 0, L \gg 1$, which is effectively a 1D problem. Whereas above ST random initial conditions led to a spiral, below ST a defect with the core surrounded by a shock structure was usually obtained for $t \to \infty$. This stationary solution exists also above ST and is reminiscent of defects trapped inside shock structures in 2D simulations after symmetry breaking. The curve ST determined in this manner is consistent with 2D simulations.

The case of negative diffusion ($\varepsilon < 0$, $|\varepsilon| \ll 1$) is important especially for lasers with negative detuning [4,21]. Then higher-order corrections to the diffusion (fourth derivative) have to be included to stabilize the short-wave instability. Our analysis shows that for $|\varepsilon| \ll 1$ the meandering is not saturated either. Presumably one has the acceleration instability of optical vortices in a wide parameter range of Maxwell-Bloch-type equations where the CGLE is invalid. Experiments with lasers (or passive systems) in the large Fresnel number range and initially a small number of vortices would be desirable.

We have benefited from discussions with S. Popp and O. Stiller. One of us (I.A.) wishes to thank the Alexander-von-Humboldt Stiftung, the Wolfson and the Rashi Foundations for research fellowships, and the University of Bayreuth for its hospitality. Support by Deutsche Forschungsgemeinschaft (SFB 213, Bayreuth) and GIF is gratefully acknowledged.

[1] See, e.g., A.C. Newell, Lect. Appl. Math. **15**, 157 (1974); Y. Kuramoto, *Chemical Oscillations, Waves and Turbulence*, Springer Series in Synergetics Vol. 19 (Springer, Berlin, 1984).
[2] P.C. Hohenberg and M. Cross, Rev. Mod. Phys. **65**, 851 (1993); A.C. Newell, T. Passot, and J. Lega, Annu. Rev. Fluid Mech. **25**, 399 (1993).
[3] F.T. Arecchi, G. Giacomelli, P.L. Ramazza, and S. Residori, Phys. Rev. Lett. **65**, 2531 (1990); **67**, 3749 (1991); M. Bramabilla, F. Battipede, L.A. Lugiato, V. Penna, F. Prati, C. Tamm, and C.O. Weiss, Phys. Rev. A **43**, 5090 (1991).
[4] G.-L. Oppo, G. D'Alexandro, and W. Firth, Phys. Rev. A **44**, 4712 (1991); P. K. Jakobsen, J. V. Moloney, A. C. Newell, and R. Indik, Phys. Rev. A **45**, 8129 (1991).
[5] A. C. Newell and J. V. Moloney, *Nonlinear Optics* (Addison-Wesley, New York, 1992).
[6] P. Coullet, L. Gil, and F. Rocca, Opt. Commun. **73**, 403 (1989).
[7] I. Aranson, L. Aranson, L. Kramer, and A. Weber, Phys. Rev. A **46**, 2992 (1992).
[8] P.S. Hagan, SIAM J. Appl. Math. **42**, 762 (1982).
[9] W. van Saarlos and P.C. Hohenberg, Physica (Amsterdam) **56D**, 303 (1992).
[10] I. Aranson, L. Kramer, and A. Weber, Phys. Rev. E **47**, 3231 (1993).
[11] D. Barkley, "Euclidean Symmetry and the Dynamics of Rotating Spiral Waves" (to be published).
[12] S. Sasa and T. Iwamoto, Phys. Lett. A **175**, 289 (1992).
[13] S. Popp, O. Stiller, I. Aranson, A. Weber, and L. Kramer, Phys. Rev. Lett. **70**, 3880 (1993).
[14] I. Aranson, L. Kramer, and A. Weber, "The Theory of Motion of Spiral Waves in Oscillatory Media," Proceedings of NATO Workshop, Santa Fe, 1993 (to be published).
[15] J. A. Sepulchre and A. Babloyantz, Phys. Rev. E **48**, 187 (1993).
[16] P. Coullet, L. Gil, and J. Lega, Phys. Rev. Lett. **62**, 1619 (1989).
[17] L. Gil, J. Lega, and J. L. Meunier, Phys. Rev. A **41**, 1138 (1990).
[18] I. Aranson, L. Kramer, and A. Weber, Phys. Rev. E **48**, R9 (1993).
[19] G. Huber, P. Alstrøm, and T. Bohr, Phys. Rev. Lett. **69**, 2380 (1992); A. Karma, Phys. Rev. Lett. **71**, 1103 (1993).
[20] H. Chaté, Nonlinearity (to be published).
[21] K. Staliunas, Phys. Rev. A **48**, 1573 (1993).

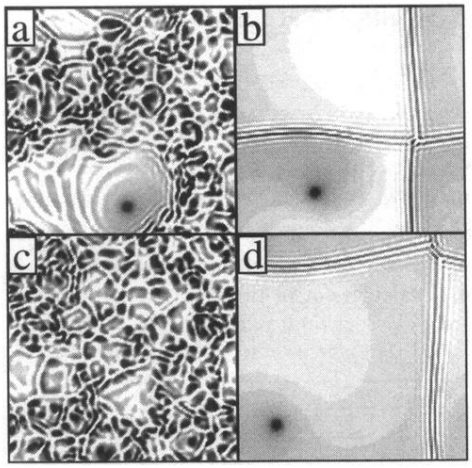

FIG. 3. Snapshots of $|A(x,y)|$ in the intermittency range for four consecutive times [$c = -0.5, \varepsilon = 0.025$; black: $|A(x,y)| = 0$; white: $|A(x,y)| = 1$]. The times corresponding to (a), (b), (c), and (d) are indicated in Fig. 2 .